Polymer Chemistry

Impact of building block structure on ion transport in cyclopropenium-based polymerized ionic liquids

Journal:	*Polymer Chemistry*
Manuscript ID	PY-ART-03-2019-000396.R1
Article Type:	Paper
Date Submitted by the Author:	06-May-2019
Complete List of Authors:	Paren, Benjamin; University of Pennsylvania, Materials Science and Engineering Raghunathan, Ramya; Columbia University, Chemistry Knudson, Isaac; Columbia University, Chemistry Freyer, Jessica; Columbia University, Chemistry Campos, Luis; Columbia University, Chemistry Winey, Karen; University of Pennsylvania, Materials Science and Engineering

Impact of building block structure on ion transport in cyclopropenium-based polymerized ionic liquids

Benjamin A. Paren[1], Ramya Raghunathan[2], Isaac J. Knudson[2], Jessica L. Freyer[2] Luis M. Campos*[2], Karen I. Winey*[1]

Abstract:

Ion transport and morphology are studied in cationic polymers based on tris(dialkyl)aminocyclopropenium ions tethered onto polystyrene (PS-TAC) and a Cl^- counterions. To investigate how molecular structure impacts single-ion transport and physical properties, the alkyl substituents on TAC were varied. Modifying the polarity, along with the size and flexibility of the functional groups on TAC significantly changes the glass transition temperature. Ionic conductivity of the PS-TAC with branched functional groups is 1-2 orders of magnitude lower than more compact and bulkier moieties on polymers at their glass transition temperature, T_g. Decreasing the size of the alkyl substituents correlates with increasing ionic conductivity in the polymers with non-polar functional groups. However, it is the geometry of the functional groups on the cation (isopropyl, ring, or linear) in PS-TAC that has a much larger effect on conductivity than the size of the group itself. Mimicking the transport properties of ionic liquids using polymers imbued with mechanical stability is essential for the development of robust, non-volatile electrolytes for batteries and fuel cells. Changing a number of variables in this tunable PS-TAC system is a step towards developing soft materials design rules for selecting solid ion supports.

[1]University of Pennsylvania, Department of Materials Science & Engineering, Philadelphia, Pennsylvania 19104, United States
[2]Columbia University, Department of Chemistry, New York, New York 10027, United States

*corresponding authors, e-mail: winey@seas.upenn.edu and lcampos@columbia.edu

Introduction

Ionic liquids (ILs) have been used for decades as a standard in state-of-the-art batteries, but have a number of drawbacks, including electrochemical instability, volatility, and poor transference number[1,2]. Some of these issues may be minimized with solid polymer electrolytes (SPEs), especially with single-ion conductors[3,4]. However, there are challenges with SPEs, particularly reaching the high ion transport levels of traditional ionic liquids. Polymerized ionic liquids (PILs) are a class of SPEs that are being explored as promising polymer electrolytes as a result of not needing additional salt solutions to be added as compared to conventional poly (ethylene oxide) based SPEs[2]. Optimizing the electrochemical benefits of ILs with the enhanced mechanical stability of a polymer backbone has the potential to create a mechanically robust, non-volatile electrolyte for batteries or fuel cells[5–7].

A large body of work has been reported on imidazolium-based PILs, with varying degrees of pendant lengths and anionic groups.[8,9,18,19,10–17] Recent work has examined how changing the counterion in a polymer containing a tris(dialkyl)aminocyclopropenium cation tethered to a polystyrene backbone (PS-TAC) affected the ion conductivity as well as structure of the polymer[20]. That study illustrated that the Cl^- counterion system has the highest conductivity at the glass transition temperature, T_g, of all the counterions examined, in part due to its small size. The cationic PS-TAC system is tunable and can be modified with different functional groups. This study investigates how changing the functional group chemistry affects the ion transport and morphology in PS-TAC polymers with a Cl^- counterion. Correlating these properties in these anion-conducting systems establishes a fundamental understanding of how the PS-TAC cation affects the ion motion, and this is a critical step in developing design parameters for PILs that may serve as polyelectrolytes.

In order to investigate the influence of the molecular structure of the building blocks, we designed a series of polymers shown in **Figure 1**, having functional groups that mainly vary in degree of branching (PS-TAC[EtOMe], PS-TAC[Bu]) and bulkiness (PS-TAC[iP], PS-TAC[Mo], PS-TAC[Pip], PS-TAC[DiMePip], PS-TAC[CyHex]). We postulate that subtle changes in the molecular structure will impact the mesoscale, and importantly, bulk thermal and ion transport properties.

Experimental

Materials

A family of [PS-TAC][Cl] polymers was prepared by a post polymerization functionalization method, reported in the literature[21–23] starting from commercially available vinyl benzyl chloride (see **Figure S1** for reaction schematics**)**. Vinyl benzyl chloride on reacting with methyl amine at 45 ºC results in vinyl benzyl methyl amine, followed by protection with the tert-butyloxycarbonyl (BOC) group. The BOC-protected monomer was polymerized by atom transfer radical polymerization (ATRP)[24]. This is followed by BOC-deprotection to unveil the secondary amine, which is subsequently reacted with the functionalized cyclopropenium chloride derivative[23] to result in library of PS-TAC.

The polymers used in this study are shown in **Figure 1**. There are five [PS-TAC][Cl] polymers that vary with steric hindrance from the size of the functional groups: isopropyl (iP), and four ring-containing groups, morpholine (Mo), piperidine (Pip), dimethyl piperidine (DiMePip), cyclohexyl (CyHex). The other two PS-TAC polymers are short-branched and flexible: ethyl oxide methyl (EtOMe), and butyl (Bu). The ^{1}H NMR spectra of these polymers is found in the supplemental information, **Figures S2-S8**.

Sample preparation

Samples were prepared from 10-15 wt% of as-received polymer dissolved in acetone (EtOMe, Bu) or methanol (Mo, Pip, DiMePip, CyHex). Solutions were then drop cast onto Teflon or steel electrodes, and left for the solvent to evaporate in air for several hours. The films were then vacuum annealed at 120-150°C (depending on glass transition temperature) for 12-24 hours.

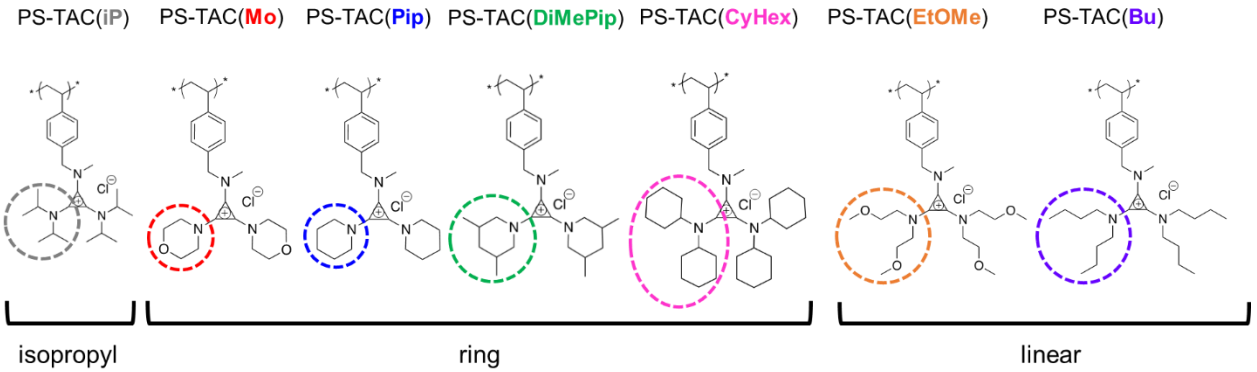

Figure 1. Chemical structures of the [PS-TAC][Cl] systems.

Temperature Modulated Differential Scanning Calorimetry (TMDSC)

For all of the [PS-TAC][Cl] systems, 4-10mg of as-annealed polymer film was kept sealed in a DSC pan for testing in a TA instruments QA 1000 differential scanning calorimeter. Samples were heated at 10ºC/min to150°C (170°C for Mo), and cooled to 20°C (0°C for EtOMe) at 5°C/min, using a modulation rate of +/- 1˚C/min . This cycle was repeated at least twice for each sample, and the second cooling was used to determine glass transition temperature (T_g). Heat flow plots for each of these polymers are found in Figure S9.

X-ray scattering

Multi-angle X-ray scattering was used to determine morphology and ion correlation distances of the [PS-TAC][Cl] films. Copper Kα X-rays (λ = 1.54 Å) were generated by a Nonius FR591 rotating anode source operated at 45kV and 60 mA. 2D scattering patterns were collected with a Bruker Hi-Star multi-wire area detector at a sample to detector distance of 11 cm (wave vector range q = 1– 16nm^{-1}). Raw 2-D scattering data was collected for 90 minutes per sample, then was azimuthally integrated into 1-D patterns for analysis.

Electrical Impedance Spectroscopy (EIS)

As-cast [PS-TAC][Cl] films were placed on a steel electrode and heated to 20°C above T_g (EtOMe, Bu), then a top electrode was pressed down onto the polymer, with 100µm silicon separators. For Pip, DiMePip, CyHex, and Mo, films were cast directly onto stainless steel electrodes, and the solvent allowed to evaporate at room temperature, with 50-100µm spacers. The sandwich of polymer between electrodes was placed into a cryostat, and equilibrated under vacuum at 400K (EtOMe, Bu) or 430K (Mo, Pip, DiMePip, CyHex) for 12 hours, to ensure any remaining solvent was removed, and maximum wetting of the polymer with the electrode interface. The measurements were performed using Solartron Modulab XM materials test system in the frequency window 10^{-1} –10^{6} Hz under an applied 0.5 V. The polymers were measured every 5°C, upon cooling, with the initial temperature varying depending on the polymer, dwelling for 20 minutes at each temperature before measurement to let the polymer equilibrate. Measurements on some systems were also conducted upon heating to ensure reversibility of the polymer systems.

Impedance spectra were fit with an equivalent circuit model (a parallel combination of a resistor and a constant phase element in series with the high-frequency resistance) to determine the through-plane high-frequency resistance R, which is used to calculate the through-plane conductivity, $\sigma_{DC} = \frac{L}{A*R}$, where L is film thickness and A is the cross sectional area. A representation of impedance data is shown in **Figure S10**.

Table 1. Van der Waals volume and glass transition temperature of different (PS-TAC)(Cl) polymers.

Functional Group	V_{vdW} (nm^3)	D_{vdW} (nm)	Tg (K)	Tg (ºC)
iP	0.33	0.85	356	83
Mo	0.25	0.78	413	140
Pip	0.27	0.80	374	101
DiMePip	0.34	0.86	397	124
CyHex	0.48	0.97	401	128
EtOMe	0.36	0.88	303	30
Bu	0.39	0.91	318	45

Results and Discussion

Differential Scanning Calorimetry

Temperature modulated differential scanning calorimetry was used to characterize the glass transition temperature of these polymers. Changing the cation in the system results in a range of glass transition temperatures from 303K to 413K depending on the chemistry (**Table 1,** heat flow plotted in **S5**). In previous work on polymerized ionic liquids, where the counterion is modified, glass transition temperature often decreases with increasing the size of the cation pair.[12] In the [PS-TAC][Cl] polymers, the glass transition temperature varies more with the polarity: Mo, is the most polar and has the highest T_g; bulkiness: CyHex is the bulkiest and has the highest T_g of the non-polar units; and branching: both EtOMe and Bu render flexibility onto the sidechains (**Figure 2**). By plotting the Van der Waals Volume (V_{vdW}) of the different TAC groups as a function of T_g (with V_{vdW} calculated as a sum of atomic and bond contributions), it is clear that the size does not directly impact the thermal properties (see Table 1 for sizes and Figure 2 for thermal properties).[25,26]

The [PS-TAC][Cl] systems with linear functional groups (EtOMe and Bu) have the lowest T_g (30-45ºC), due to their flexible nature. Interestingly, the similarity of these branches to polyethylene and poly (ethylene oxide), which have much lower T_g than a rigid polymer like polystyrene,[27,28] could explain the dramatic difference in T_g from the ring-based PILs. The steric hindrance caused by the rigid, bulky functional groups in Mo, Pip, DiMePip, and CyHex [PS-TAC][Cl] result in the highest glass transition temperatures (101-140ºC). The oxygen atoms in the Mo groups result in stronger dipolar interactions in Mo than Pip, leading to the difference in T_g of 40ºC between the two systems. Without added polarity, the T_g of the ring-based PILs

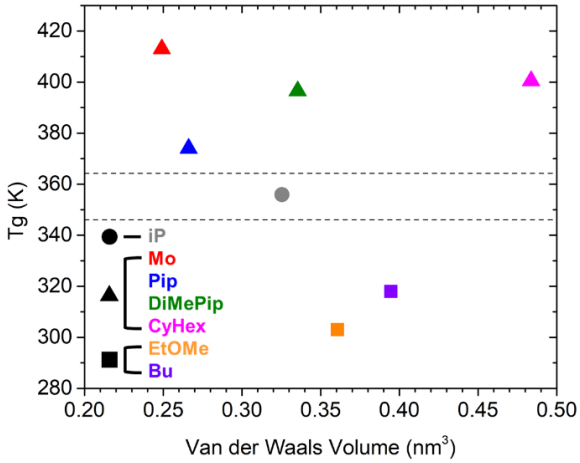

Figure 2. Glass transition temperature vs. V_{vdW} of the PS-TAC polymers. The systems are separated into isopropyl (●), ring-based (▲), and linear (■) functional groups. Data for iP from Ref. 20.

(Pip, DiMePip, and CyHex) increases with V_{vdW}, which is expected because larger functional groups would further limit mobility of the polymer. The T_g of Pip is nearly identical to PS (~100ºC)[29], perhaps a result of the fact that it has two rings off of the TAC cation. The glass transition of the iP system lies in between the linear and ring-based [PS-TAC][Cl] (Tg=83ºC), with the rotational freedom of the isopropyl groups allowing for more mobility than the rigid heterocycles.

Morphology

Three main correlation peaks are present in room temperature X-ray scattering data of the [PS-TAC][Cl] polymers (**Figure 3**). These peaks were fit to Lorentzian functions to determine their positions, width, and intensity (**Figure S11**). The peak at ~7.5nm^{-1}, q_i, represents the distance between neighboring cationic (or anionic) groups.[8,9,13,20,30–32] The correlation length associated with each peak, d_x, is calculated using the equation $d_x=2\pi/q_x$. d_i, the distance between cationic groups, ranges from 0.71nm (iP) to 0.88nm (CyHex) in the [PS-TAC][Cl] polymers.

In PILs, the polarity alternation between the polar functional groups and nonpolar backbone leads to a nanophase separation. The low q peak in Figure 3a (~3nm^{-1}), q_b, is associated with this nanophase separation, and corresponds to the backbone-to-

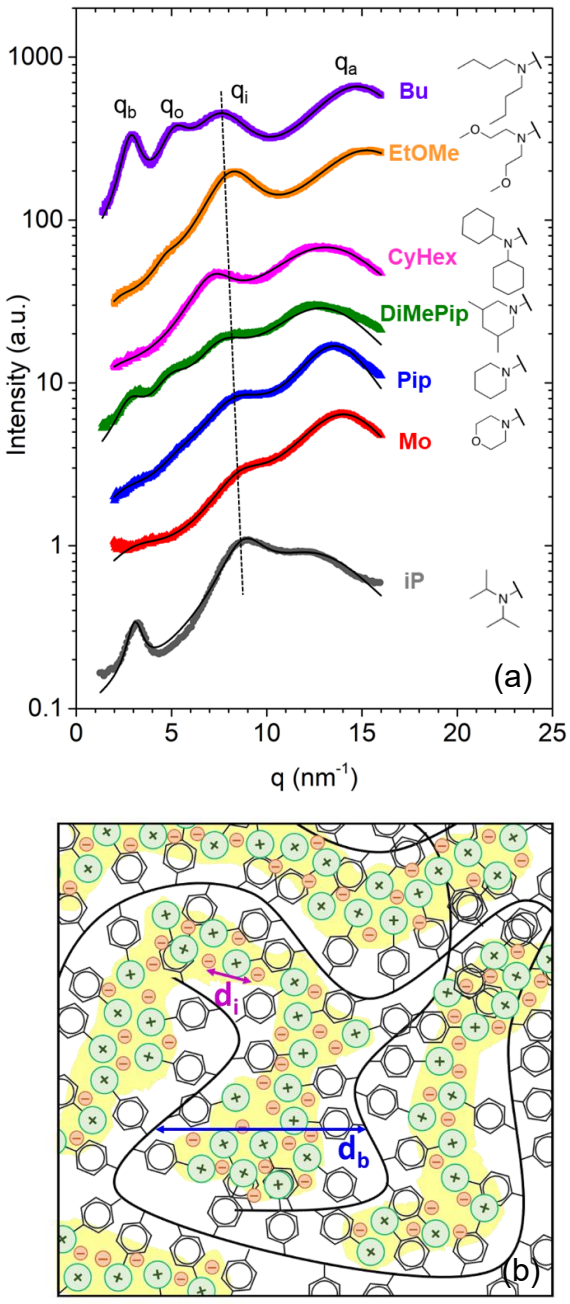

Figure 3. (a) X-ray scattering patterns and fits of all the PS-TAC PILs. Data for iP from Ref. 20. (b) Schematic representation of d_i and d_b.

backbone distance in the polymer melt.[8,9,20,30–32] The length-scale of this ordering is 2.04-2.98nm (**Table S1**), which is a realistic backbone-backbone distance based on the polystyrene backbone in [PS-TAC][Cl] and size of the cations. The intensity and breadth of this peak, which are associated with the degree of nanophase separation, varies depending on the functional group, with no clear trend. The combination of geometry, size, polarity, and flexibility of the different functional groups may hinder polar-nonpolar structural organization in some of the [PS-TAC][Cl] systems, affecting the characteristics of q_b.

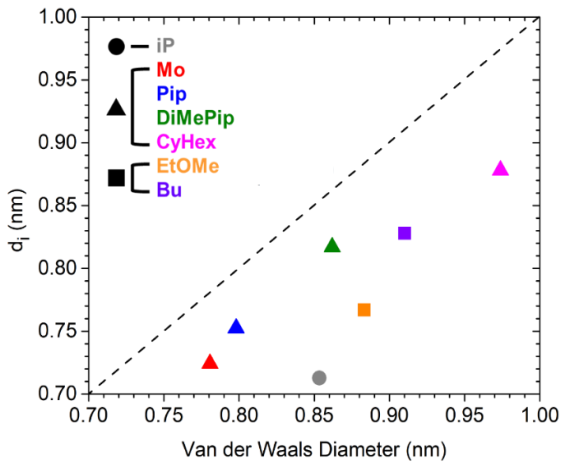

Figure 4. Comparison of calculated VDW diameter with measured cation-cation distance. The dashed line represents $d_i=D_{vdW}$.

The correlation length q_a, the amorphous halo, is generally attributed to the interactions between pendant groups in PILs, but in this case is also attributed to small-scale interactions between the backbone polymer and cation-anion pairs.[10,20] In all of the [PS-TAC][Cl] systems, q_a appears relatively unchanged with varying cation, and is nearly identical in value to neat polystyrene (q_a = 13 nm^{-1}). Several of the PILs exhibit a fourth ordering peak, q_o, at q~5nm^{-1}. The appearance and size of this peak is variable in the polymers and has not yet been identified in this system, but is attributed to ordering of the functional groups on the length scale of ~1.1nm. The presence of ordering peaks beyond q_a, q_i, and q_b, has been demonstrated in other PIL systems in literature,[33] but is not of primary interest in this study because there is, no apparent correlation between the presence of this peak and the ionic conductivity.

The V_{vdW} of Cl^- is 5-10% of the size of the TAC cations investigated,[20] so d_i must be dominated by the cation size, with little impact from the anion. Furthermore, because the only variable changing between the different X-ray patterns is the chemistry of the cation group, we interpret that the change in d_i is a direct result of the change in cation size. This is supported by a comparison of the estimated Van der Waals (D_{vdW}) diameter to d_i of each [PS-TAC][Cl] systems in **Figure 4**. The calculation of D_{vdW} from V_{vdW} is $D=(6V/\pi)^{1/3}$ and assumes a spherical geometry of the cation and no changes in the free volume, which is a simplification for the anisotropic TAC cations. Although these assumptions overestimate D_{vdW}, there is a clear positive correlation between D_{vdW} and d_i. The ring-based functional groups most closely follow the trend of $d_i=D_{vdW}$, and varying behavior between types of functional groups may be due to differences in stacking and free volume of the groups in the amorphous matrix.

Ion Conductivity

Electrical impedance spectroscopy was used to determine the ionic conductivity (σ_{DC}) of the [PS-TAC][Cl] polymers (**Figure 5**). Because the [PS-TAC][Cl] systems are single ion-conductors, the ion transport is dominated by the anion. Realistically, as the polymer moves, the tethered cation will contribute to the total ion transport, but it is expected to be orders of magnitude lower than the anion, and its contribution is ignored in this analysis.

The ionic conductivities vary significantly between [PS-TAC][Cl] systems as a function of 1/T, **Figure 5a**. The variation in conductivity between the PILs at a specific temperature arises from the significant differences in T_g between the polymers. The materials with lower T_g have the highest conductivity at a specific

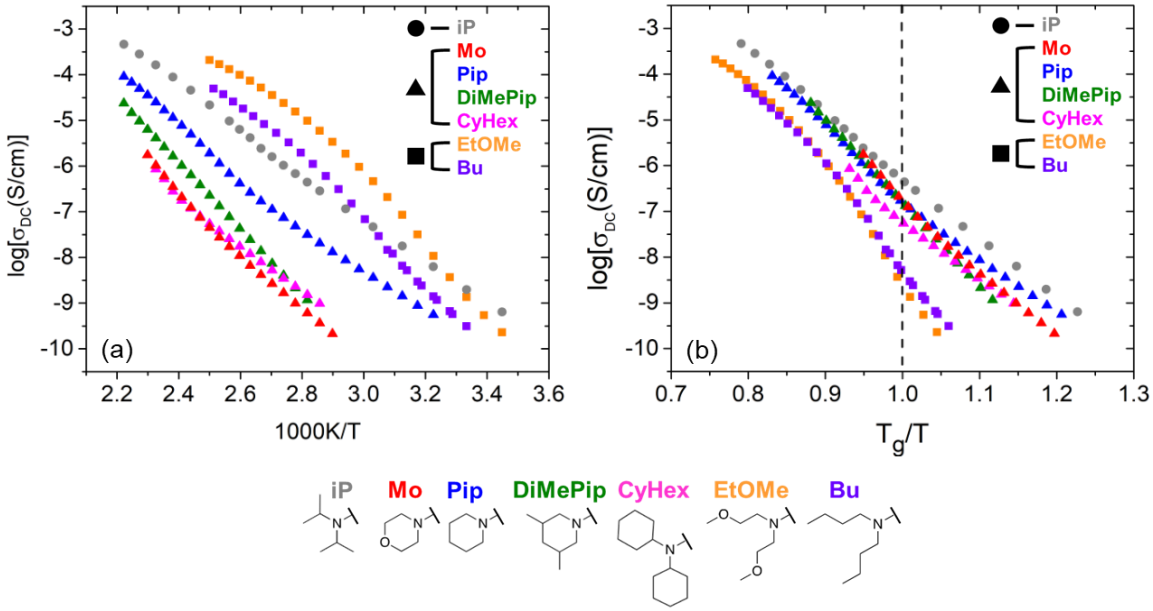

Figure 5. Plots of (a) DC conductivity versus inverse temperature and (b) DC conductivity versus Tg/T for the [PS-TAC][Cl] polymers. Data for iP taken from Ref. 20.

temperature, because polymer dynamics are faster at the same temperature in lower T_g materials and the primary mechanism for ion transport is coupled with segmental motion.

Above T_g, Vogel-Fulcher-Tamman (VFT) behavior is observed in the conductivity, most prominently in the systems with linear functional groups. A desirable property of a mechanically robust electrolyte is high conductivity at and below the glass transition, which is the region of greatest interest in this study. **Figure 5b** illustrates the temperature-normalized conductivity, where the [PS-TAC][Cl] iP system has the highest conductivity, ~10^{-6} S/cm, at T_g. The ring-based cations have conductivity within an order of magnitude below this. The linear functional group systems (Bu and EtOMe), exhibit conductivity of ~10^{-8}-10^{-9} S/cm at T_g, significantly lower conductivity than the non-linear systems. All of the systems exhibit Arrhenius behavior below T_g, suggesting the dominant mechanism of transport to be Cl^- ions hopping between cationic sites, as opposed to the VFT mechanism of moving with segmental dynamics.[34] VFT and Arrhenius fits of the data in Figure 5 can be found in the supporting information section (**Figure S12**).

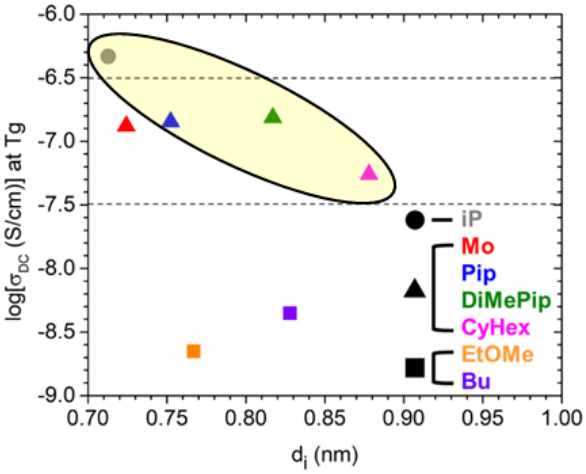

Figure 6: DC conductivity at Tg/T=1 vs. d_i at 298K. The systems are separated into isopropyl (●), ring-based (▲), and linear (■) functional groups. The highlighted region represents the functional groups without added polarity or linear geometry (iP, Pip, DiMePip, CyHex).

In literature, conductivity is frequently correlated with morphology in imidazolium based PILs, with changing pendant group length and anionic group. [10,16–18] Recent work illustrated that increasing pendant group length with the TFSI counterion results in an increased d_b and a reduced DC conductivity.[10] We are investigating how changing the cation affects conductivity not only as d_b changes, but also as d_i changes due to different functional group chemistries in [PS-TAC][Cl]. The ion transport takes place when the Cl^- moves between cationic groups along the same polymer chain, with an average jump distance d_i, as well as hopping between cationic groups on different chains, with an average jump distance, d_b.[25]

The variation in the breadth and intensity of q_b in Figure 3a, as well as the peak positions, suggest no clear correlation between d_b and the ionic conductivity of the [PS-TAC][Cl] polymers. This departure from literature, where increasing d_b results in lower conductivity, is likely since d_b is changing as a function of cation geometry, size, and polarity, in the PS-TAC systems as opposed to just the distance between the cations.

The [PS-TAC][Cl] polymers containing non-polar functional groups that strictly vary in bulkiness ([small] iP < Pip < DiMePip < CyHex [large]) demonstrate a reduction in conductivity as d_i increases (**Figure 6**). For ion diffusion through ion conductors in the glassy state, the activation energy for ion hopping can be described by $E_a = \frac{a_0^2 v_0^2 m_{ion}}{2}$, where a_0, v_0, and m_{ion} are the jump distance, oscillation frequency, and mass of the anion, respectively.[25,26,33] Since $\sigma_{DC} = \sigma_0 e^{\frac{-E_a}{RT}}$ in the Arrhenius regime, it is expected that the conductivity would increase as the jump distance, in this case d_i, decreases, which is the case with these [PS-TAC][Cl] systems. The activation energy for ion hopping of these polymers is found in **Table S2**.

The most significant impact on the conductivity is not the size of the functional group, but rather the geometry and polarity of the cations, which may explain why Mo, EtOMe, and Bu diverge from the trend exhibited by the other systems. iP (with isopropyl geometry) has the highest conductivity, and the ring-based PS-TACs are all 0.5-1 orders of magnitude lower. The branching of the Bu and EtOMe functional groups may result in reduced free volume compared to iP and the ring-based polymers when the chains are less mobile below the glass transition temperature. The reduction in free volume could limit the mobility of Cl^-, leading to a conductivity at the glass transition temperature 1-2 orders of magnitude lower than the isopropyl and ring geometries.

Furthermore, conductivity may also be reduced by added polarity to the functional group, caused by the presence of oxygen that leads to stronger dipoles. These dipoles can add to the energy barrier for hoping between cationic sites. This phenomenon is evident between the Mo and Pip systems, in which Mo cations are closer together, but exhibit lower conductivity than Pip. Similarly, the conductivity of EtOMe is half an order of magnitude lower than Bu, even though EtOMe has closer cation centers, which could be a function of geometry, but also of the dipoles introduced by the oxygen in the functional group.

The limited change in conductivity with the functional group chemistry in PS-TAC could be a consequence of the cyclopropenium cation's extreme bulkiness. This can hinder the mobility of the polymer to rearrange itself in such a way to favor ion transport. Large functional groups may block the ion from interacting with cationic charge centers. While the charge itself is delocalized, functional groups that are too large may present physical barriers for the anionic charge to dissociate from one cation and move to the next.

Although the presence and position of a backbone-backbone peak do not appear to correlate with DC conductivity in the [PS-TAC][Cl] polymers, the report of this correlation in the imidazolium bromide polymer system, as well as the existence of the correlation with cation-cation distance with conductivity in the PS-TAC systems, suggest further ways to tune PIL systems.

Whether that is by functionalizing the cationic groups in the imidazolium bromide system or changing the pendant group length in the PS-TAC system, there are endless possibilities to tune PILs that may result in higher conductivities with mechanically stable polymer systems.

Conclusion

A set of [PS-TAC][Cl] polymerized ionic liquids with different functional groups on the cation were synthesized via a post polymerization functionalization method. The functional groups varied in size, polarity, and geometry. Solid polymer films were produced from these PILs and characterized with differential scanning calorimetry, X-ray scattering, and electrical impedance spectroscopy to examine the effects of morphology and chemistry of the functional groups on ionic conductivity. The PILs exhibited glass transition temperatures from 303-413K depending on the functional group, and all demonstrated Arrhenius ion transport behavior below T_g. There was significant variation in the morphology of the PILs, particularly regarding the degree of nanophase ordering. The distance between cationic centers was dominated by the cation, due to the large size difference with the chloride anion. There was a slight reduction in conductivity with increasing cation size for the PS-TACs with nonpolar, non-linear functional groups, but the most significant changes in conductivity were a result of geometry, with the isopropyl and ring functional groups having conductivity 1-2 orders of magnitude higher than the linear systems. Overall, we examined a variety of functional group geometries, sizes, and polarities with the PS-TAC system, but the bulky TAC cation appeared to limit the conductivity that could be reached in these polymers. Changing a number of variables in this tunable PS-TAC system provides insights toward developing fundamental design rules for highly conductive polymer electrolytes based on PILs.

Acknowledgements

B. A. P. and K.I.W. acknowledge funding from the National Science Foundation (NSF) DMR 1506726, and NSF PIRE 1545884. L.M.C. acknowledges support from the National Science Foundation (NSF CAREER DMR-1351293).

Conflicts of interest

There are no conflicts of interest to declare.

References

(1) Armand, M.; Endres, F.; MacFarlane, D. R.; Ohno, H.; Scrosati, B. Ionic-Liquid Materials for the Electrochemical Challenges of the Future. *Nat. Mater.* **2009**, *8* (8), 621–629.

(2) Shaplov, A. S.; Marcilla, R.; Mecerreyes, D. Recent Advances in Innovative Polymer Electrolytes Based on Poly(Ionic Liquid)S. *Electrochim. Acta* **2015**, *175*, 18–34.

(3) Matsumi, N.; Sugai, K.; Miyake, M.; Ohno, H. Polymerized Ionic Liquids via Hydroboration Polymerization as Single Ion Conductive Polymer Electrolytes. *Macromolecules* **2006**, *39* (20), 6924–6927.

(4) Chemistry, P. Received 6 May 1985; in Revised Form Received 10. **1985**, *17*, 307–311.

(5) Hayes, R.; Warr, G. G.; Atkin, R. Structure and Nanostructure in Ionic Liquids. *Chem. Rev.* **2015**, *115* (13), 6357–6426.

(6) Tang, M. H.; Savage, A. M.; Li, C. Y.; Beyer, F. L.; Nykaza, J. R.; Elabd, Y. A.; Wang, S.; Pan, Q. Polymerized Ionic Liquid Diblock Copolymer as Solid-State Electrolyte and Separator in Lithium-Ion Battery. *Polymer (Guildf).* **2016**, *101*, 311–318.

(7) Meek, K. M.; Sun, R.; Willis, C.; Elabd, Y. A. Hydroxide Conducting Polymerized Ionic Liquid Pentablock Terpolymer Anion Exchange Membranes with Methylpyrrolidinium Cations. *Polymer (Guildf).* **2018**, *134*, 221–226.

(8) Choi, U. H.; Ye, Y.; Salas De La Cruz, D.; Liu, W.; Winey, K. I.; Elabd, Y. A.; Runt, J.; Colby, R. H. Dielectric and Viscoelastic Responses of Imidazolium-Based Ionomers with Different Counterions and Side Chain Lengths. *Macromolecules* **2014**, *47* (2), 777–790.

(9) Liu, H.; Paddison, S. J. Direct Comparison of Atomistic Molecular Dynamics Simulations and X-Ray Scattering of Polymerized Ionic Liquids. *ACS Macro Lett.* **2016**, *5* (4), 537–543.

(10) Iacob, C.; Matsumoto, A.; Brennan, M.; Liu, H.; Paddison, S. J.; Urakawa, O.; Inoue, T.; Sangoro, J.; Runt, J. Polymerized Ionic Liquids: Correlation of Ionic Conductivity with Nanoscale Morphology and Counterion Volume. *ACS Macro Lett.* **2017**, *6* (9), 941–946.

(11) Fan, F.; Wang, Y.; Hong, T.; Heres, M. F.; Saito, T.; Sokolov, A. P. Ion Conduction in Polymerized Ionic Liquids with Different Pendant Groups. *Macromolecules* **2015**, *48* (13), 4461–4470.

(12) Cheng, Y.; Yang, J.; Hung, J.-H.; Patra, T. K.; Simmons, D. S. Design Rules for Highly Conductive Polymeric Ionic Liquids from Molecular Dynamics Simulations. *Macromolecules* **2018**, acs.macromol.8b00572.

(13) Delhorbe, V.; Bresser, D.; Mendil-Jakani, H.; Rannou, P.; Bernard, L.; Gutel, T.; Lyonnard, S.; Picard, L. Unveiling the Ion Conduction Mechanism in Imidazolium-Based Poly(Ionic Liquids): A Comprehensive Investigation of the Structure-to-Transport Interplay. *Macromolecules* **2017**, *50* (11), 4309–4321.

(14) Evans, C. M.; Bridges, C. R.; Sanoja, G. E.; Bartels, J.; Segalman, R. A. Role of Tethered Ion Placement on Polymerized Ionic Liquid Structure and Conductivity: Pendant versus Backbone Charge Placement. *ACS Macro Lett.* **2016**, *5* (8), 925–930.

(15) Keith, J. R.; Mogurampelly, S.; Wheatle, B. K.; Ganesan, V. Influence of Side Chain Linker Length on Ion-Transport Properties of Polymeric Ionic Liquids. *J. Polym. Sci. Part B Polym. Phys.* **2017**, *55* (23), 1718–1723.

(16) Morgan, B. F.; Beyer, F. L.; Chen, T.-L.; Elabd, Y. A.; Sun, R.; Willis, C. Lithium Ion Conducting Polymerized Ionic Liquid Pentablock Terpolymers as Solid-State Electrolytes. *Polymer (Guildf).* **2018**, *161* (December 2018), 128–138.

(17) Bartels, J.; Sanoja, G. E.; Evans, C. M.; Segalman, R. A.; Helgeson, M. E. Decoupling Mechanical and Conductive Dynamics of Polymeric Ionic Liquids via a Trivalent Anion Additive. *Macromolecules* **2017**, *50* (22), 8979–8987.

(18) Runt, J.; Price, T. L.; Lee, M.; Choi, U. H.; Colby, R. H.; Gibson, H. W.; Mittal, A. Molecular Volume Effects on the Dynamics of Polymerized Ionic Liquids and Their Monomers. *Electrochim. Acta* **2014**, *175*, 55–61.

(19) Schneider, Y.; Modestino, M. A.; McCulloch, B. L.; Hoarfrost, M. L.; Hess, R. W.; Segalman, R. A. Ionic Conduction in Nanostructured Membranes Based on Polymerized Protic Ionic Liquids. *Macromolecules* **2013**, *46* (4), 1543–1548.

(20) Griffin, P. J.; Freyer, J. L.; Han, N.; Geller, N.; Yin, X.; Gheewala, C. D.; Lambert, T. H.; Campos, L. M.; Winey, K. I. Ion Transport in Cyclopropenium-Based Polymerized Ionic Liquids. *Macromolecules* **2018**, *51* (5), 1681–1687.

(21) Freyer, J. L.; Brucks, S. D.; Gobieski, G. S.; Russell, S. T.; Yozwiak, C. E.; Sun, M.; Chen, Z.; Jiang, Y.; Bandar, J. S.; Stockwell, B. R.; et al. Clickable Poly(Ionic Liquids): A Materials Platform for Transfection. *Angew. Chemie - Int. Ed.* **2016**, *55* (40), 12382–12386.

(22) Brucks, S. D.; Freyer, J. L.; Lambert, T. H.; Campos, L. M. Influence of Substituent Chain Branching on the Transfection Efficacy of Cyclopropenium-Based Polymers. *Polymers (Basel).* **2017**, *9* (3).

(23) Jiang, Y.; Freyer, J. L.; Cotanda, P.; Brucks, S. D.; Killops, K. L.; Bandar, J. S.; Torsitano, C.; Balsara, N. P.; Lambert, T. H.; Campos, L. M. The Evolution of Cyclopropenium Ions into Functional Polyelectrolytes. *Nat. Commun.* **2015**, *6*, 1–7.

(24) Matyjaszewski, K.; Xia, J. Atom Transfer Radical Polymerization. *Chem. Rev.* **2001**, *101* (9), 2921–2990.

(25) Salas-De La Cruz, D.; Green, M. D.; Ye, Y.; Elabd, Y. A.; Long, T. E.; Winey, K. I. Correlating Backbone-to-Backbone Distance to Ionic Conductivity in Amorphous Polymerized Ionic Liquids. *J. Polym. Sci. Part B Polym. Phys.* **2012**, *50* (5), 338–346.

(26) Zhao, Y. H.; Abraham, M. H.; Zissimos, A. M. Fast Calculation of van Der Waals Volume as a Sum of Atomic and Bond Contributions and Its Application to Drug Compounds. *J. Org. Chem.* **2003**, *68* (19), 7368–7373.

(27) Davis, G. T.; Eby, R. K. Glass Transition of Polyethylene: Volume Relaxation. *J. Appl. Phys.* **1973**, *44* (10), 4274–4281.

(28) Faucher, J. A.; Koleske, J. V.; Santee, E. R.; Stratta, J. J.; Wilson, C. W. Glass Transitions of Ethylene Oxide Polymers. *J. Appl. Phys.* **1966**, *37* (11), 3962–3964.

(29) Kawana, S.; Jones, R. A. L. Character of the Glass Transition in Thin Supported Polymer Films. *Phys. Rev. E - Stat. Physics, Plasmas, Fluids, Relat. Interdiscip. Top.* **2001**, *63* (2), 6.

(30) Araque, J. C.; Hettige, J. J.; Margulis, C. J. Modern Room Temperature Ionic Liquids, a Simple Guide to Understanding Their Structure and How It May Relate to Dynamics. *J. Phys. Chem. B* **2015**, *119* (40), 12727–12740.

(31) Liu, H.; Paddison, S. J. Alkyl Chain Length Dependence of Backbone-to-Backbone Distance in Polymerized Ionic Liquids: An Atomistic Simulation Perspective on Scattering. *Macromolecules* **2017**, *50* (7), 2889–2895.

(32) Benetatos, N. M.; Winey, K. I. Nanoscale Morphology of Poly(Styrene-Ran-Methacrylic Acid) Ionomers: The Role of Preparation Method, Thermal Treatment, and Acid Copolymer Structure. *Macromolecules* **2007**, *40* (9), 3223–3228.

(33) Heres, M.; Cosby, T.; Mapesa, E. U.; Liu, H.; Berdzinski, S.; Strehmel, V.; Dadmun, M.; Paddison, S. J.; Sangoro, J. Ion Transport in Glassy Polymerized Ionic Liquids: Unraveling the Impact of the Molecular Structure. *Macromolecules* **2018**, acs.macromol.8b01273.

(34) Petrowsky, M.; Frech, R. Temperature Dependence of Ion Transport: The Compensated Arrhenius Equation. *J. Phys. Chem. B* **2009**, *113* (17), 5996–6000.

Graphical Abstract:

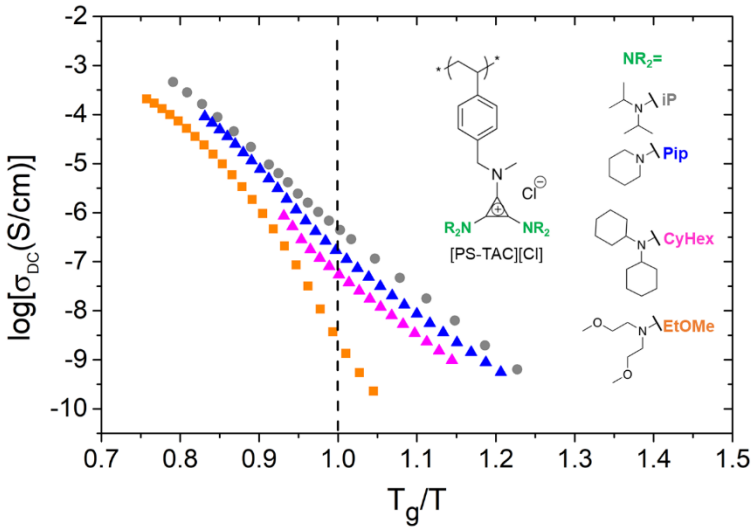

Cation geometry, size, and polarity all contribute to conductivity in PS-TAC PILs, with highest conductivity from the isopropyl cation geometry.